Observation of Water Volume Changes of Rivers in Amazon Forests from Multi-temporal JERS-1 SAR Images

Takako Sakurai-Amano and Mikio Takagi

Dept. of Applied Electronics, Science University of Tokyo

ABSTRACT

We have developed a new method to visualize river networks in tropical rain forests from JERS-1 SAR images. This method compresses river information in an original SAR image to a small image displaying wide rivers as dark objects in real size and narrower rivers as bright objects showing brightness level as an indicator of the discharge. We applied this method to 476 images of Amazon forests, 13 observations for path 415 data and 11 observations for path 416 data between 1993 and 1997. We confirmed that a change observed in a preliminary experiment was certainly a part of seasonal changes. The changes roughly correspond to the monthly precipitation changes. Through a simple digital analysis although qualitative, we also detected subtle but consistent regional differences among minor tributaries that belong to a major tributary basin.

Keywords: seasonal change, discharge, tropical rain forests, Amazon Basin, JERS-1 SAR

1. INTRODUCTION

Vegetation in tropical rain forests is rich in amounts of global biomass and in variety of species [Morley, 2000]. Rivers transport water, soil and nutrients important for growing those plants [Balek, 1983]]. L-band Space-borne Synthetic Aperture Radars (SAR) are best for regularly monitoring the water surfaces in large, often remote and cloud-covered areas, as they can observe the Earth's surface irrespective of the sun and cloud cover [Ulaby et al. 1986].

We have developed a new method of visualizing rivers in tropical rain forests. This method compressed river information in an original SAR image to a small image displaying wide rivers as dark objects in real size and narrow rivers as bright objects. In previous studies, we found the bright rivers are open-water rivers, not rivers hidden under the canopies [Sakurai-Amano, et al. 2000]. We also found that these rivers showed temporal changes [Sakurai-Amano, et al. 2001].

Encouraged by those positive results, we further continued to examine the applicability of this method by applying longer observation periods and different tropical forest areas. We modified the previous program mostly for the purpose to handle a large number of data more quickly. Then we applied this method to all available temporal data. We examined data visually and then analyzed them digitally in more details.

In this paper, we report some results obtained from the Amazon Basin.

2. MICROWAVE INTERACTION WITH RIVERS IN TROPICAL RAIN FOREST

As illustrated in Fig.1 (a) schematically, strong targets caused by corner-reflections between the water surface and trunks or large branches appear along the river lining up intermittently. While a river is wide, those strong targets are apparent against the dark river in SAR images. When the rivers become very narrow, those targets appear weaker and less frequently because part of the microwave scatters within the canopy. They are also not very apparent because the rivers are no longer very dark.

Let us consider a river in a wet season when the water level is higher. As illustrated in Fig.1 (b), more reflections are found on the narrow boundary area

because more tree trunks are in the water. Thus the brightness of a river increases as the width of open-water area and the numbers of inundated trees along the river increase. We ignored the reflections inside flooded forests beyond this narrow area because our algorithm minimized such reflections as described in section 3.

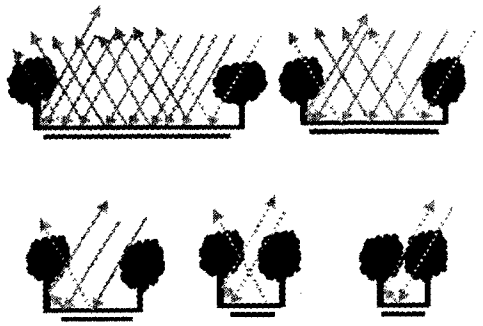

(a) reflection and river width

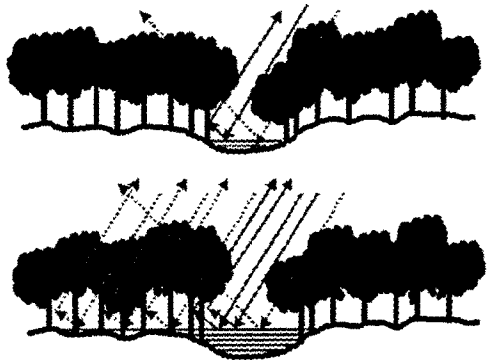

(b) dry season and wet season

Fig.1 Microwave interaction with rivers in the forest.

3. METHODOLOGY

The essence of our visualization algorithm emphasizes very bright pixels lining along the river pixels and averages them to connect each other. While river pixels are very dark, a sum of the absolute differences at a river boundary is very high, but the sum becomes lower when river pixels become less dark. In a wet season, the bright pixels become even brighter as the number of strong reflections increases within a resolution cell. Then the sum of the absolute differences will increase. There are also many more reflections within the flooded forest, but the sum of the absolute difference between a bright pixel and the surrounding bright pixels is not very large. Only bright boundary pixels along the river pixels are enhanced in this algorithm.

The detailed description of the method was found in the previous papers (Sakurai-Amano et al., 2000, 2001). Here we only describe the modifications. The first modification is to decimate the input image before speckle noise reduction. Second modification is at the size reduction (step 5). Instead of a simple decimation, we use the average of 8x8-pixel area as the pixel value of reduced image. Fig.2 shows the flow diagram.

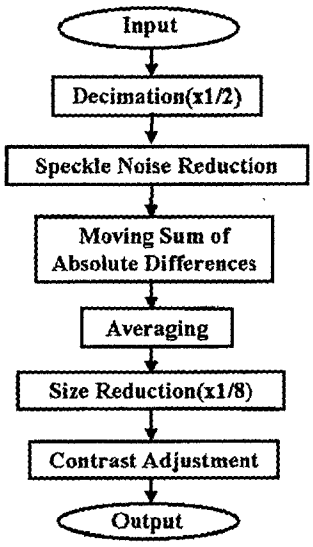

Fig.2. The flow diagram.

4. DATA

We used the level 2.1 4-look JERS-1 SAR images (©METI/NASDA)of all available temporal data for path 415 and 416 scenes (row 301 to 320).

Monthly precipitation data are the 1 degree by 1degree products of GPCC, gridded datasets of monthly total precipitation, downloaded from Deutscher Wetterdienst (http//www.dwd.de/research/gpcc/e06a .html).

5. RESULTS AND DISCUSSION

5.1 Visual observation

In almost all scenes, rivers showed a large seasonal change. For example, Fig.3 shows scene 416-312 at all observation dates. Every year rivers in April and May at near the end of rainy season appear brighter and longer

and have more tributaries. Rivers in dry August or October images showed fewer tributaries. Months of maximum and minimum water volumes in Manaus at both Negro River and Amazon Rivers show a slight delay compared to those of southern areas. We detected large changes from time to time in the most southern scenes in both paths but the change patterns did not follow the monthly precipitation patterns. Since the scenes cover not forests but agricultural areas, their patterns might be correlated with weekly or shorter-term precipitation patterns.

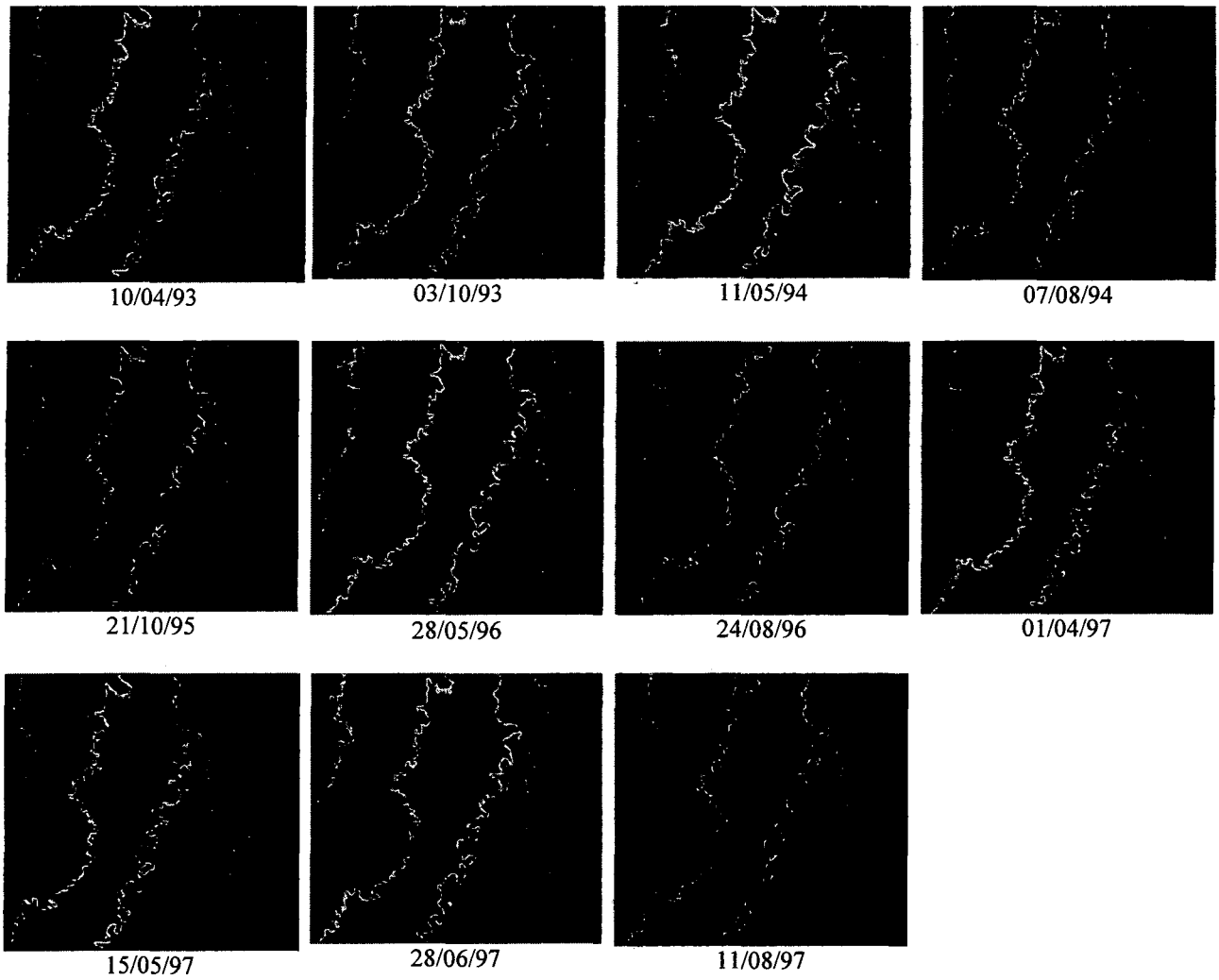

Fig.3. 416-312

5.2 Digital Analysis

With this method, we can visually detect large changes very easily. However, our eyes cannot detect subtle differences in the brightness. To examine the accuracy and consistency of the brightness levels on bright rivers, we created a simple and qualitative digital procedure to estimate discharge volume using brightness and area size of rivers. To avoid confusing objects easily, we analyzed the data interactively. The analysis was done in the following 6 steps

1) Specify interactively a rectangular area that surrounds a tributary system, a tributary or a potion of a tributary that was to be analyzed.

1) Create a binary image at a given threshold value. We selected a value between 90 and 135 common to all images of each scene observed at different dates. We usually used 90 or 100 values to avoid inundated forests, but we sometimes used higher values when other tributary, man-made objects, or hills are too close or attached to the specified

tributary at the time of higher water level.

2) Connect very closely lined-up blobs by morphological closing operation. We usually used a 3x3 squared template, but use a 5x5 circular template for very narrow rivers because they tend to be a series of linear blobs in the binary image. When there are too many branches, we did not use a template.
3) Interactively specify a small rectangular area that surrounds the downstream area of the selected tributary system.
4) Extract a river area connecting to the lowest part of the tributary selected in step 4 from the tributary system selected at step 1 (see Fig.11 and Fig.15).
5) Calculate the following value that relates to the discharge volume of extracted river area.

$$D = \sum_{Area} (z_i - F_{\max})$$

where z_i is a 16-bit pixel value, $F_{\max}$ is the pixel value at maximum of the main lobe averaged over dry season histograms of the scene and usually has a value of about 60. In this experiment, we selected moderately narrow rivers that are wider than about 50 m depending on threshold values at step 2.

We selected bright rivers in the scenes of path 415 from row 305 to 314 and path 416 from row 303 to 316.

Although the results should be compared with the discharge volumes of ground experiments at the time of the satellite observations, those ground data were not available to us. The precipitation played a relatively large role to control the discharge in tropical rain forests, if not the largest and precipitation data, monthly or long-term averages, were more widely available even they are mostly estimated values in tropical rain forest regions. Therefore we compared the results with monthly precipitations in this analysis just to see whether there was any correlation between the values estimated from SAR data and precipitations and when and where there are such correlations, if any. We were more concerned with the regional consistencies among the discharge volumes (normalized values) in neighboring scenes. We plot the monthly precipitations from GPCC products on the same graphs for comparison.

We clearly detected seasonal changes and confirmed the visual findings. The changes are so large that we see them even in extracted area. Fig.4, for example, shows the river areas of a tributary in scene 416-312 at all observation dates. We used a threshold value of 90 at step 2 and no template at step 3 to extract them. Fig.4 (l) shows a display after a rectangular area is specified at step 1. We see a rough correlation between those changes and monthly precipitation in terms of the maximum months, the minimum months and the periods. (See Fig.5).

We even detected a subtle regional differences from the Amazon data. The change patterns of tributaries in nearby scenes were similar to each other. We classified them into 5 types based on the change patterns between 1996 and 1997, a period of most frequent observations. Fig.5 plots the normalized discharge of tributaries in each type. We selected two tributaries for each type in the graph. Each type of tributaries seemed to relate to the basin of a certain major tributary. Type A belongs to the Negro basin, type B to the Amazon basin in a narrow sense, type C to the Madeira basin, type D to the Dos Marmelos basin, and type E to the upper part of Dos Marmelos basin. It is reasonable to assume that the climatic and ground conditions of tributaries that belong to such major tributary basins are similar at least within the observed area of about 150 km width and about 200 km length and hence the change patterns of discharge volumes in the same type are similar.

Center locations of precipitation data that belong to type A, B, C, D, and E areas were respectively (60.5°W, 1.5°S), (60.5°W, 3.5°S), (60.5°W, 5.5°S), (61.5°W, 7.5°S), and (61.5°W, 8.5°S).

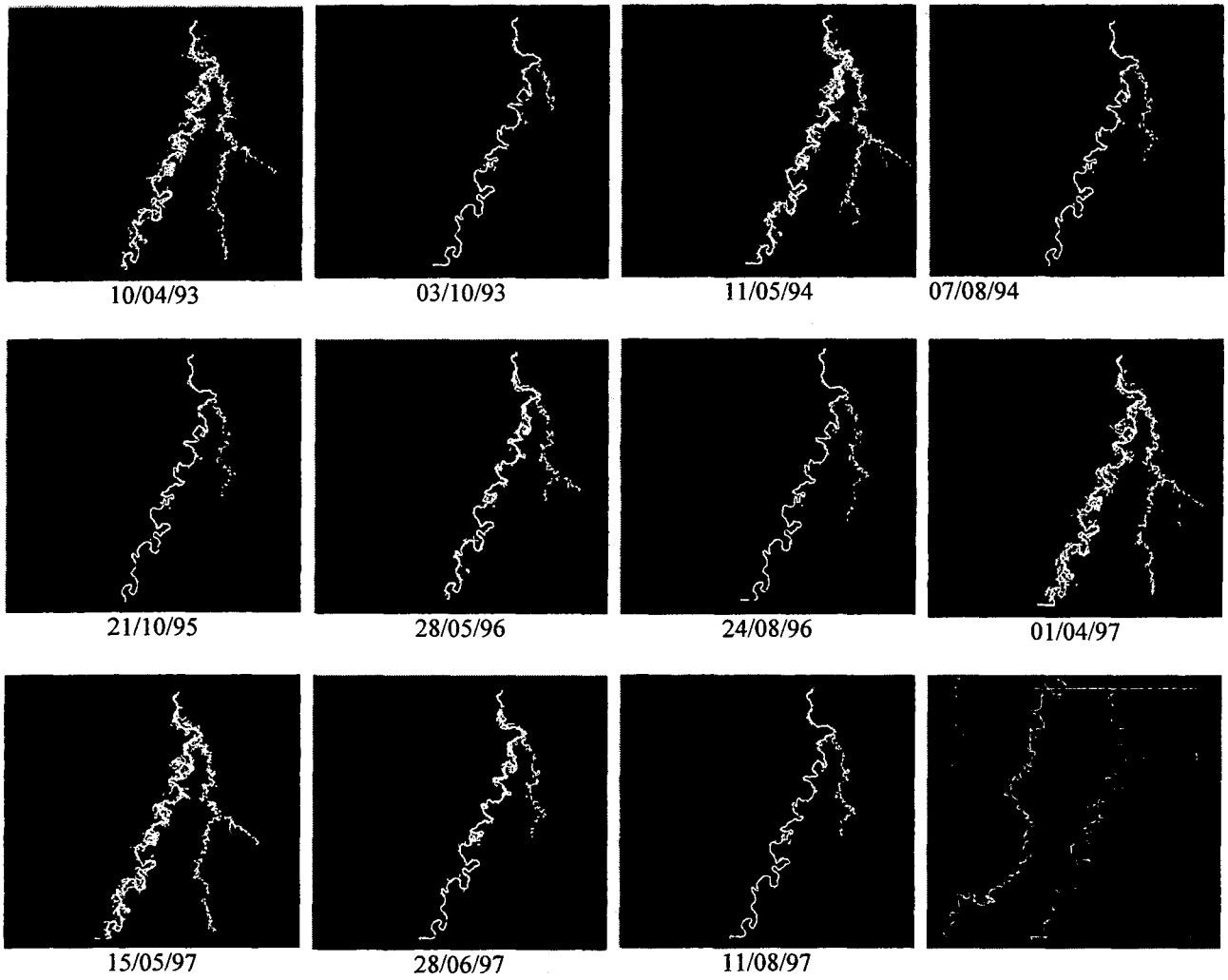

Fig.4. Extracted river area

6. SUMMARIES AND CONCLUSION

We have developed a new method for visualizing narrow rivers from JERS-1 SAR images. The method can detect the seasonal changes of the narrow open-water rivers in tropical forest areas as the brightness changes of the rivers. Since the brightness increases with the width and water level of the river, the changes can be translated into discharge volumes of the rivers. We applied the method to the rivers in Amazon forests and visually detected a large seasonal change. The seasonal change pattern of discharge volumes is roughly correlated with precipitation change pattern.

From simple interactive digital analyses, our new method not only confirmed the visual findings but also detected subtle but consistent regional differences that are common to a major tributary basin.

Satellite base measurements are very much desirable as options in huge, remote, uninhabited, and often dangerous tropical rain forest areas where ground based measurement stations are scarce. Our method could provide qualitative discharge data of moderately narrow rivers in various different tropical rain forest areas throughout the world those complements to the ground measurements. Unfortunately the number, span, frequency, and areas of JERS-1 observations are quite limited. We hope for more satellites in the future, resulting in more detailed studies. The Japanese ALOS will launch in 2004. We hope it will monitor those regions regularly and more frequently and contribute to an understanding of the water cycles in tropical rain forests.

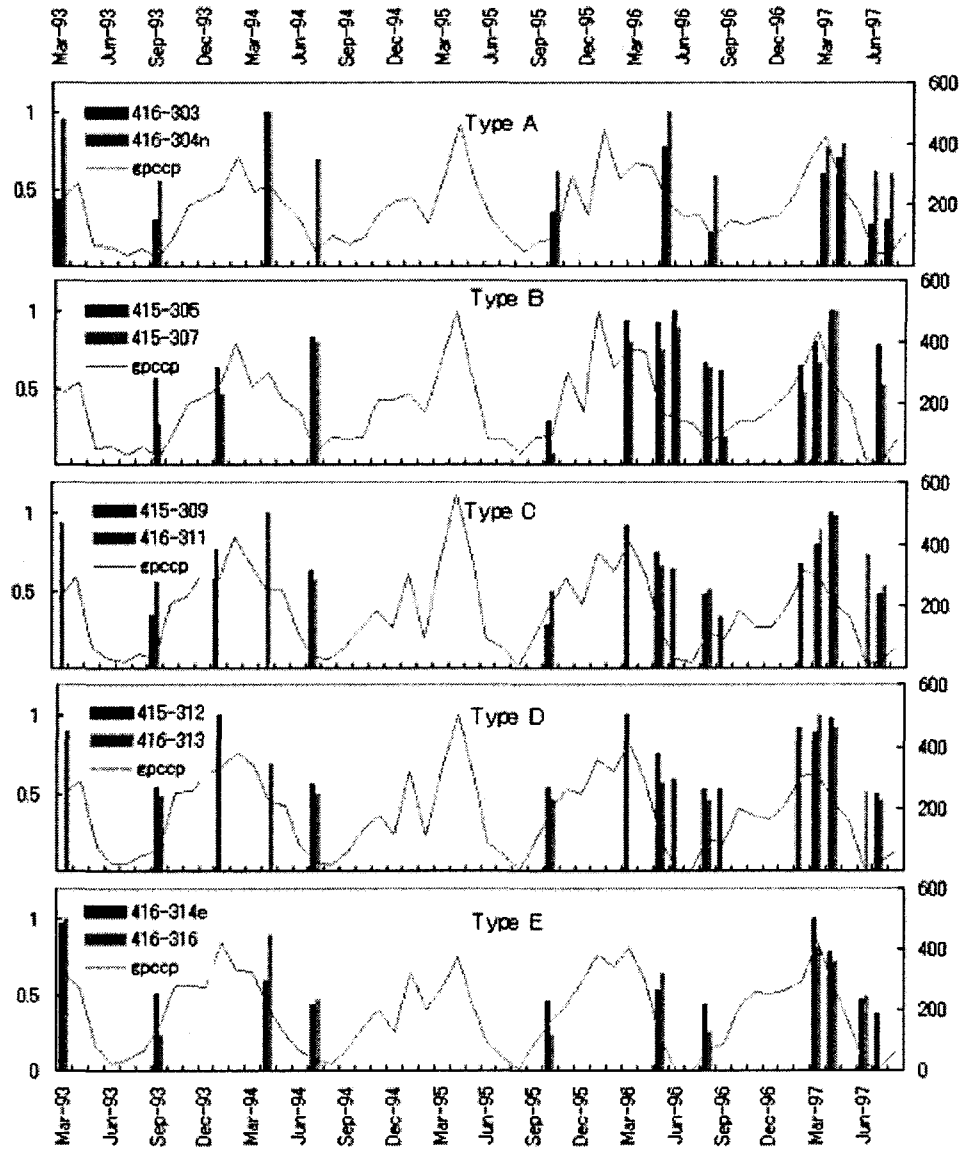

Fig.5. Various types of change patterns.

ACKNOWLEGMENT

We would like to thank K. Nakasugi, T. Yoshioka, and E. Ishida, undergraduate students at Dept. of Applied Electronics, Science University of Tokyo for processing a large number of SAR data, Prof. S. Ogawa of Rissho University for valuable suggestions, and K. Dairaku, Institute of Industrial Science, University of Tokyo for giving us the information of GCPP products..

REFERENCES

J. Balek, *Hydrology and Water Resources in Tropical Region*, Elsevier, 1983, ch.3.

R. J. Morley, *Origin and Evolution of Tropical Rain Forests*, Wiley, 2000

T. Sakurai-Amano, J. Iisaka, and M. Takagi (2000), "Detection of Narrow Open-water Channels from JERS-1 SAR Images of Amazon Forests", Proc. of SPIE, Vol.4152, pp.120-130, October, 2000, Sendai, Japan

T. Sakurai-Amano, K. Nakasugi, T. Yoshioka and M. Takagi (2001), "Detection of Seasonal Changes of Rivers in Tropical Forests from JERS-1 SAR Images of Amazon, New Guinea, and Congo Basin", Proc. of SPIE, Vol.4542-13, September, 2001, Toulouze, France

F. T. Ulaby, R. K. Moor and A. K. Fung, *Microwave Remote Sensing, Active and Passive*, Arktech House, Inc., 1986, vol.II.

Baseline Refinement for Topographic Phase Estimation using External DEM

Chang Won Lee, Wooil M. Moon

ESI[3] Laboratory, School of Earth and Environmental Sciences (SEES), Seoul National University, Seoul, 151-742, Korea (bosscq@eos1.snu.ac.kr, wmoon@eos1.snu.ac.kr)

Abstract: Multitemporal interferometric SAR has became an useful geodetic tool for monitoring Earth's surface deformation, generation of precise DEM, and land cover classification even though there still exist certain constraints such as temporal and spatial decorrelation effects, atmospheric artifacts and inaccurate orbit information. The Korea where nearly all areas are heavily vegetated, JERS-1 SAR has advantages in monitoring surface deformations and environmental changes in that it uses 4-times longer wavelength than ERS-1/2 or RADARSAT SAR system.

For generating differential SAR interferogram and differential coherence image for deformation mapping and temporal change detection, respectively, topographic phase removal process is required utilizing a reference interferogram or external DEM simulation. Because the SAR antenna baseline parameter for JERS-1 is less accurate than those of ERS-1/2, one can not estimate topographic phases from an external DEM and the residual phase appears in differential interferogram.

In this paper, we examined topographic phase retrieval method utilizing an external DEM. The baseline refinement is carried out by minimizing the differences between the measured unwrapped phase and the reference points of the DEM.

1. Introduction

Multitemporal SAR interferometry has became an useful geodetic tool for generation of high precision DEM and monitoring Earth surface changes such as earthquake deformation, sea ice movement, volcano inflation and land subsidence [1]. In addition coherence imagery can be used for random surface change detection and environmental process monitoring [4,6]. In Korea where most regions except urban areas are heavily vegetated and highly humid, the JERS-1 L-band SAR system has definite advantages over the C-band system in that it is less sensitive to temporal decorrelation caused by various surface changes. For detecting ground deformation from measured SAR phase information or unbiased coherence estimation, topographic phase must be removed. The 2-pass method utilizes external DEM instead of an interferogram for topographic phase removal. One of the merits of the 2-pass methods is that the DEM coregistered to the radar coordinate can be regarded as many GCPs and that manual human intervention can be minimized.

Inaccurate baseline parameters calculated from JERS-1 orbit ephemeris result in residual fringe patterns in differential interferograms. In the case of ERS-1/2 which uses more accurate orbit information than JERS-1 or RADARSAT, baseline refinement is required.

Baseline refinement is carried out in two steps. First, a simulated interferogram is generated from the DEM using an initial baseline parameter. Second, the relation between the measured unwrapped phase of the interferogram and the reference phase computed from the DEM is used for correcting baseline after building baseline model.

2. Methodology

Interferogram simulation method

For the generation of topographic phase from a reference DEM, the input DEM must be resampled and registered to the master radar coordinate. Using the following relation between the radar geometry and DEM,